Arab J. Nucl. Sci. Appl., Vol. 54, 2, 50-62 (2021)

ISSN 1110-0451

Arab Journal of Nuclear Sciences and Applications

Web site: esnsa-eg.com

(E S N S A)

Mg-Cr Layered Double Hydroxide (LDH) Intercalated with Sodium Dodecyl Sulfate as Sorbent for Alizarine Red-S in Aqueous Solutions

I.M. Ahmed[a, b]

[a]*Chemistry Department, College of Science, Jouf University, Sakaka, Saudi Arabia*
[b]*Hot Laboratories and Waste Management Center, Egyptian Atomic Energy Authority,Cairo, Egypt*

ARTICLE INFO

Article history:
Received: 24th Sep. 2020
Accepted: 24th Dec. 2020

Keywords:
Sorption,
Alizarine Red-R,
LDH,
Surfactant.

ABSTRACT

Mg^{2+}/Cr^{3+}-LDH, ($LDH-CO_3$) with Mg/Cr molar ratio 2.0 and intercalated LDH with an anionic surfactant, sodium dodecyl sulphate, SDS-LDH were synthesized by co-precipitation method and was used for the sorption of Alizarine Red-S (ARS) as anionic organic dye. The prepared adsorbents were characterized by FTIR, XRD, TGA and surface area. The influence of pH of the medium, shaking time, dye concentration and adsorbents dose on the sorption process were investigated. The kinetics of the sorption process was estimated using the pseudo first-order, pseudo second-order, intra particle diffusion and Elovich kinetic model. The results of $LDH-CO_3$ fitted well with the pseudo -first-order model while the pseudo -second-order model fitted with SDS-LDH results. The obtained results indicated that the intercalation with SDS enhanced the sorption process and can be considered as a promising adsorbent for the removal of anthraquinone compounds from wastewater. Regeneration of the adsorbent was achieved using 0.1 M sodium hydroxide solution.

INTRODUCTION

Pollution control is one of the important environmental issues in the world. Large quantities of dyes that are produced from many industries as leather tanning, paints, paper, pharmaceuticals and food are discharged in the water streams. Fifteen percent of the total dyes produced annually are released in the water streams during textiles industries. As the dyes are non-biodegradable and cause the coloration of water which prevents the penetration of light in the water systems causing hazardous effects to all aquatic living organisms as most of them are carcinogenic and mutagenic [1-3]. Many techniques were applied for the removal of dyes as ozonation [4], electrocoagulation [5, 6], photo-degradation [7], aerobic and anaerobic biodegradation [8-10], biosorption [11], ion exchange [12], solvent extraction [13], oxidation [14] and precipitation [15] however, these techniques have some drawbacks as dyes are tailored to be resistant to degradation and even the degradable species may be more toxic and not economically feasible. Adsorption is an effective method for dye removal due to the ease, efficient and low cost operation. Many adsorbents were investigated for the removal of cationic and anionic dyes using low cost adsorbents as natural clays that are generally hydrous aluminosilicate with high surface areas and high cation exchange [1]. The most used clays as adsorbents are montmorillonite and kaolinite group clays with the general formula of $Al_2Si_2O_5(OH)_4$ [16], industrial wastes as metal hydroxide sludge [17, 18], red mud [19-21], zerovalent iron [22], activated carbon [23], organoclay [24] and biosorbent materials [25-27]. The layered double hydroxides (LDHs) have a general formula $[M_{1-x}^{2+} M_x^{3+} (OH)_2 A_{x/n}^{-} \cdot mH_2O]$, where M^{2+} is a divalent cation, $M^{3+}$is a trivalent metal cation and A^{n-} is the interlayer anion that are found on the surface and/or in the interlayer spaces. Several methods were proposed for the preparation of LDH as co-precipitation, hydrothermal methods and mechanochemical synthesis

Corresponding author: ismadwy@yahoo.ca
DOI: 10.21608/ajnsa.2020.43981.1405

etc. Many factors affect the synthesis of LDHs by co-precipitation as the pH, precipitation method, precipitation temperature, reagent concentration, aging and the presence of impurities [28]. The surface and interlayer anions and water molecules can be exchanged with other inorganic and organic anions from contaminated waters [29]. LDHs were used as adsorbents for the removal of heavy metals, radionuclides, oxyanions [30-33], dyes [34-40]. Intrercalation using organic surfactants to increase the hydrophobicity have found many applications in the removal of organic materials from industrial wastewater.

Anthraquinone compounds have many applications in dyes, metallochrome indicators, drugs, or staining the biological samples. From these dyes, Alizarin Red S (9,10-dihydro-3,4-dihydroxy-9,10-dioxo-2 anthracenesulfonic acid) (ARS) that is commonly used in staining calcium deposits in tissues, in geology to stain and differentiate carbonate minerals, ARS is used as spectrophotometric determination of some elements of nuclear interest as uranium [41], Zirconium [42], Aluminum [43], etc., and in dyeing textiles, such dye cannot be completely degraded by the above mentioned methods due to its complex structure and its thermal and optical stability. For these reasons, this category of dyes attract attention of researchers to find a simple and low cost technique for the removal of ARS.

In this paper, the possibility of using LDH-CO_3 and SDS-LDH for the sorption behavior of ARS from aqueous solution has been investigated in order to examine the effect of intercalation on the sorption process.

2. EXPERIMENTAL

2.1 Materials and methods

Alizarine- Red S was used as delivered by the supplier (Riedl-de Haen,). Magnesium chloride hexahydrate, chromium(III) chloride hexahydrate, sodium carbonate were purchased from Merck. For all experiments, double distilled water was used.

2.2 Synthesis of the adsorbents

2.2.1 LDH-CO_3

LDH-CO_3 was synthesized by the co-precipitation method using $MgCl_2 \cdot 6H_2O$ and $CrCl_3 \cdot 6H_2O$. The Mg:Cr molar ratio of 2:1 was obtained by using 0.1 mol/L Mg^{2+} and 0.05 mol/L Cr^{3+}. 100.0 mL of 2.0 M Na_2CO_3 was added dropwise to 100.0 mL of the above mentioned mixture that stirred for 18 h and the pH was maintained in the range of 10±0.1. The final greenish blue precipitate was aged for 24 h at 80 ^oC, then filtered, washed with distilled water and dried at 60 ◦C overnight.

2.2.2 SDS-LDH

0.5 g of sodium dodecylsulfate (SDS) in 100 mL of distilled water was stirred with 5.0 g of (LDH-CO_3) for 1.0 h at 353 ^oK in air. The suspension was then centrifuged and the solid was washed three times with hot distilled water and dried at 338 ^oK overnight, Fig.1 represents schematic structure of both LDH-CO_3 and SDS-LDH.

2.3 Instrumentation

UV–Visible Recording Spectrophotometer (Cary 60, Agilent, USA) was used for estimation of ARS concentration. FT-IR spectra of LDH-CO_3 and SDS-LDH before and after sorption were recorded at a wavelength range of 400-4000 cm^{-1} by Fourier Transform Infra-red Spectrometer (FTIR)IR-Tracer 100, Shimadzu, Japan. The pore structure and surface area were examined by nitrogen adsorption/desorption at 77^oK using a gas sorption analyzer (Quantachrome, NOVA 4200 e series, USA). The thermal stability of the adsorbent was investigated by a Shimadzu, TGA 51-thermal analyzer, at heating rate of 10 ^oC/min. XRD pattern of the adsorbent was measured using CuKα radiation by Shimadzo X-Ray powder diffractometer (XRD 7000) within 2θ ranging from 10 to 80^o.

2.4 Sorption of ARS onto LDH-CO_3 and SDS-LDH

0.05 g of the adsorbents were equilibrated with 10 mL of 100 mg/L of ARS for 60.0 min. at pH 6.0, and the solution was centrifuged for ARS measurement by UV-Vis spectrophotometer at 555.0 nm . The percent uptake (uptake %) was calculated by the following equation:

$$uptake\,\% = \frac{C_o - C_e}{C_o} \times 100 \qquad \textbf{(1)}$$

The adsorption capacity of ARS, qe (mg/g), was calculated according to the equation:

$$q_e = (C_o - C_e)\frac{V}{m} \qquad \textbf{(2)}$$

where Co, Ce are the initial and equilibrium ARS concentration in (mg/L), V and m are the volume of the solution (L) and the mass of adsorbent (g), respectively.

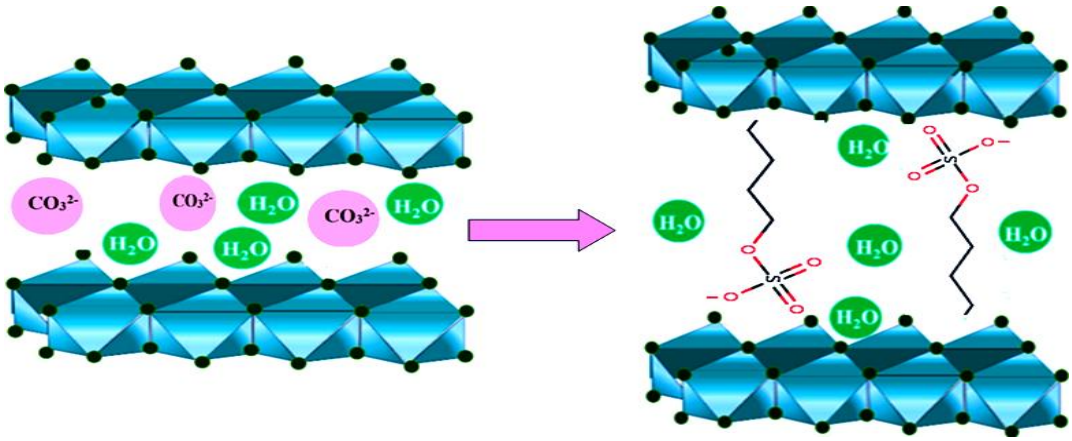

Fig. (1) Schematic structure of both LDH-CO_3 and SDS-LDH

3 RESULTS AND DISCUSSION

3.1 Characterization of the adsorbent

FT-IR spectra of LDH-CO_3, SDS (LDH), ARS and dye-loaded adsorbent are shown in Fig. 2. The spectrum of LDH-CO_3 shows the characteristic absorption bands of a hydroxyl group, at 3390 cm^{-1} due to the hydration of water molecules and OH groups of brucite like structure [29]. The band at 1446, 1367 and 873 vibration of interlayer CO_3^{2-} cm^{-1}. In the SDS-LDH bands at 2900, 2800 cm^{-1} C-H stretch vibration bands are due to CH_3 and CH_2 group, C-H bending vibration appears at 1400 cm^{-1}. Loaded LDHs spectra show bands in the range of about 450 to 650 cm-1 which are due to O–M–O, M–O–M and M–O–H lattice vibrations [44], ARS shows peaks at 1665 and 1637 cm^{-1} that are referred to C=O stretching vibration, the peaks at 1589 cm^{-1} are due to the C=C bonds in benzene ring and the bands at 1439 , 1220, 1068 and 1150 cm^{-1} are referred to the sulfonic groups[45, 46].

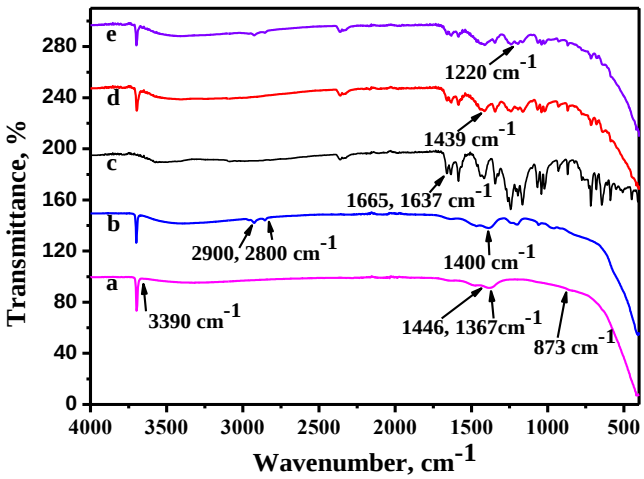

Fig. (2): FT-IR of Cl-LDH and SDS-LDH. [a- LDH-CO_3; b- SDS-LDH; c- ARS; d- LDH-CO_3-ARS; e- SDS-LDH-ARS]

The XRD pattern of LDH-CO_3 and SDS- LDH are represented in Fig. 3. exhibit some common features of LDH, three intense lines at low 2θ angle corresponding to diffraction by planes (003), (006) and (009) and the peak between 60 and 63° (2θ) is due to (110) plane [47]. After anionic exchange with CO_3, the d_{003} plane peak was shifted towards lower 2θ value from 11.529° to11.455 An increase of basal spacing from 7.67 to 7.72 Å was observed, also the average crystallite size was calculated by Scherrer's equation and found to be 5.42 and 5.0 nm for LDH-CO_3 and SDS- LDH, respectively.

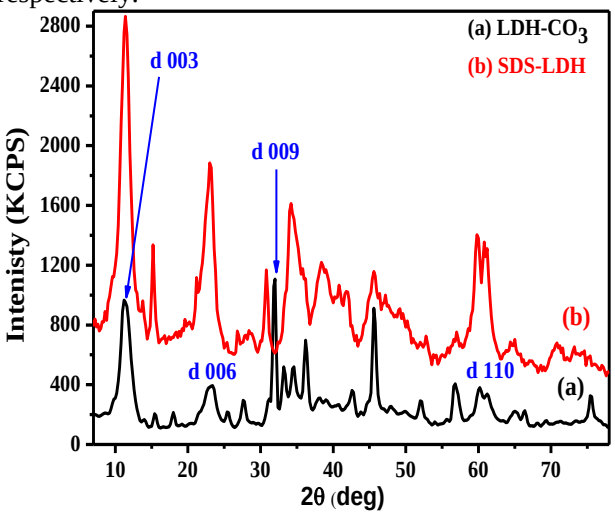

Fig. (3): XRD of LDH-CO_3 and SDS-LDH

The BET surface area of LDH-CO_3 and SDS-LDH were 72.49 and 62.87 m^2/g. Thermogravimetric analysis,TGA of LDH-CO_3 and SDS-LDH up to 600 °C are shown in Fig. 4. The weight loss in the range 25-300 °C was nearly equal to 16.6 and 15.7 % may be due to loss of surface adsorbed and interlayer water, while the

weight loss in the range 300-450 was 14.8 and 20.5% for LDH-CO_3 and SDS-LDH, respectively due to dehydroxylation from the inorganic layers [48] which indicates that the intercalation of the surfactant does not significantly change the thermal stability of the sorbents.

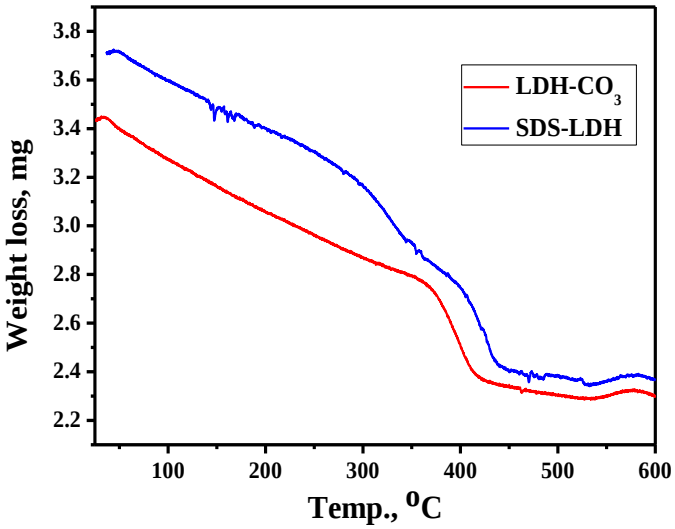

Fig. (4): TGA for LDH-CO_3 and SDS-LDH

3.2 Effect of pH on the removal of ARS

The pH is a critical factor in the sorption process as it affects the surface charges of adsorbents, leading to the electrostatic interactions between the adsorbent and adsorbate[49]. As the pH< pHpzc, the surface of the adsorbent gains a positive charge and enhances the uptake of ARS due to the electrostatic attraction force and when the pH > pHpzc, the negatively charged adsorbent could oppose the sorption process. The effect of pH on the adsorption of ARS onto LDH-CO_3 and SDS-LDH was carried out in the range (2.0- 10.0) with a V/m ratio 200 mL/g, Fig. 5. It is clear that the sorption of Alizarine Red -S remained constant in the range 2.0-8.0 then decreased with increasing the pH of the aqueous solution. Even at higher pH between 8.0 and 10.0, a sorption process was observed which indicates that there is that another interaction, such as complexation, is the primary interaction between LDH-CO_3 or SDS-LDH and ARS. Also at pH >8.0 the ionization of phenolate group that acquires a negative charge on the dye surface was observed [50]. Fig. 6 represents the formula of ARS in extended conformation. All investigations were carried out at pH 6.0 where the predominant species are the neutral species AH_2 and the anionic one AH^- [51] that enhances the electrostatic interaction with the positively charged surface of the adsorbents [52]. The possible interactions between LDH-CO_3 or SDS-LDH and ARS dye are proposed in Fig.7.

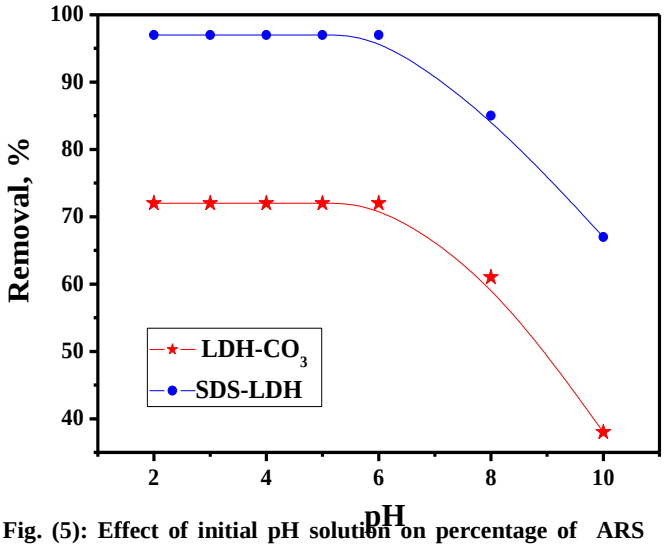

Fig. (5): Effect of initial pH solution on percentage of ARS removal onto LDH-CO_3 and SDS-LDH: V/m = 200 mL/g, T: 25±1°C, [ARS] = 100 mg/L

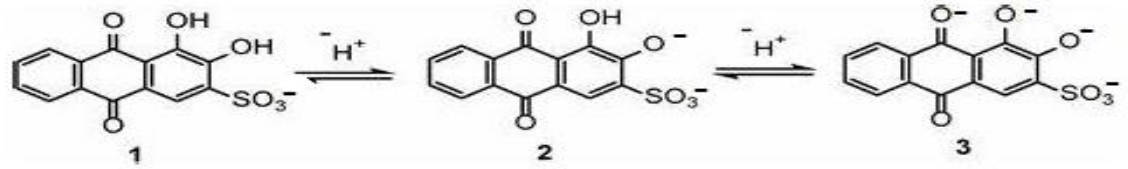

Fig. (6): Formula of ARS in extended conformation

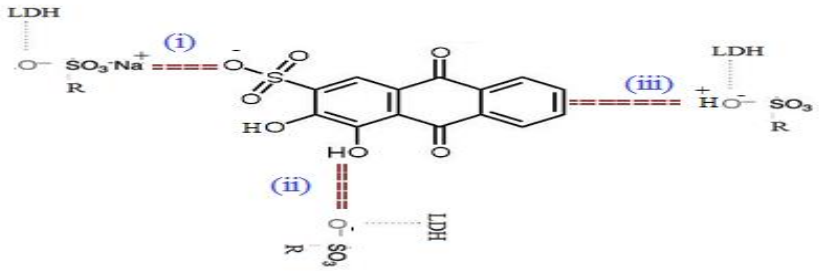

Fig. (7): The SDS-LDH and ARS dye interaction. (i)ionic interaction between SDS-LDH-dye at pH 6; (ii) Hydrogen bond between SDS-LDH-dye ; (iii) Hydrogen bond between SDS-LDH and aromatic residue in the dye

3.3 Effect of sorbent dose

The effect of LDH-CO_3 and SDS-LDH dose on the sorption of Alizarine Red -S ions was investigated in the range 0.01-0.05 g/10.0 mL solution with 100 mg/L of Alizarine Red -S at ambient temperature (25°C) for 30.0 min. As seen from Fig. 8, the percent uptake of ARS increased with increasing the sorbent dose due to the increase in the number of active sites available for adsorption [53]. In this respect 0.05 g/10.0 mL that corresponds to a V/m ratio 200 mL/g was used in this investigation.

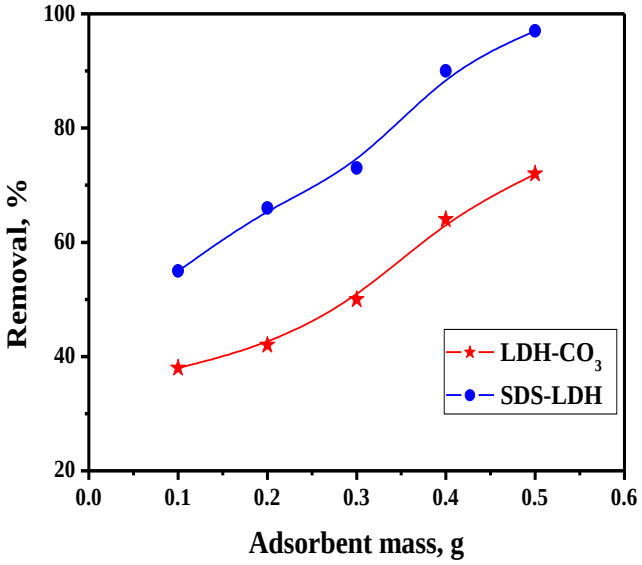

Fig. (8): Effect of adsorbent dose on percentage of ARS removal onto LDH-CO_3 and SDS-LDH: pH: 6, T: 25±1°C, [ARS] = 100 mg/L

3.4 Sorption kinetics

The effect of contact time on the sorption of ARS was investigated in the range between 3.0 and 60.0 min. using ARS concentration of 100 mg/L onto LDH-CO_3 and SDS-LDH with a V/m ratio 200 mL/g, Fig. 9. The equilibrium established within 30.0 min. and the intercalation with the surfactant enhanced the uptake of the dye from 72 to 97% .

Four kinetic models were examined to set the order of the sorption. The pseudo- first order kinetic model was estimated according to the equation:

$$\log(q_e - q_t) = \log q_e - (\frac{k_1}{2.303})t \qquad (3)$$

Where k_1 is the rate constant of pseudo- first- order (min^{-1}). The values of k_1 and q_e can be calculated from the slope and intercept on plotting log (q_e-q_t) versus (t), Fig. 10 and are reported in Table (1, 2). It is clear that the results fit the model in case of LDH-CO_3 system.

The sorption data were investigated by pseudo-second - order mechanism according to the equation (4):

$$\left(\frac{t}{q_t}\right) = \left(\frac{1}{k_2 q_e^2}\right) + \left(\frac{1}{q_e}\right) t \qquad (4)$$

Where k_2 (gmg^{-1} min^{-1}) is the rate constant of the second-order adsorption. The equation constants can be determined by plotting t/q_t against t, Fig. 11, and the results are tabulated in Table (1, 2). The regression coefficient (R^2) was around 0.996. It is clear that the data obtained fit this model as the values of q_{exp} are similar to $q_{cal.}$ for SDS-LDH system.

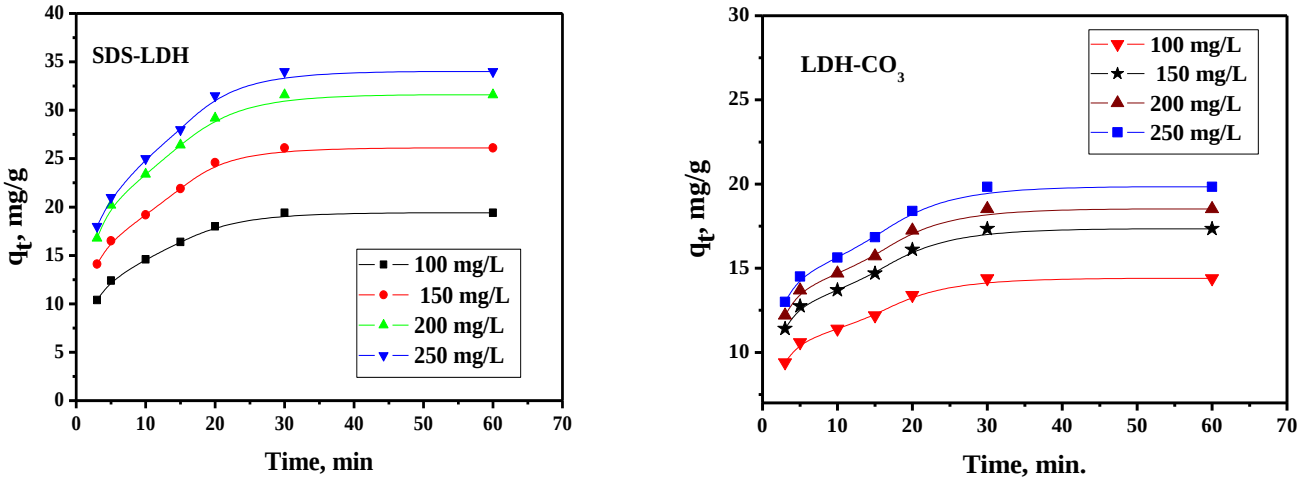

Fig. (9): Effect of contact time on percentage of ARS removal onto LDH-$CO_3$and SDS-LDH: V/m = 200 mL/g , pH: 6, T: 25±1°C, [ARS] = 100 mg/L

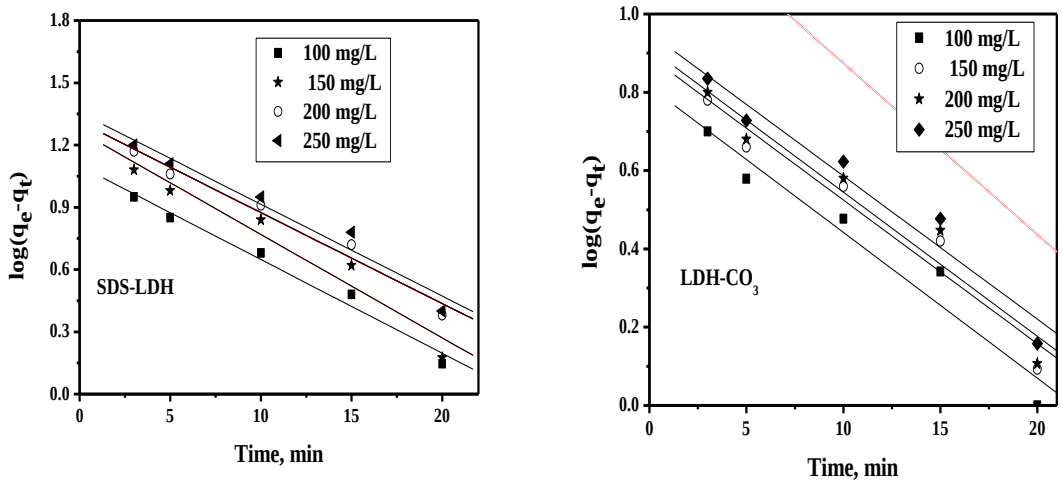

Fig. (10): First order Kinetic model for adsorption of ARS onto LDH-CO_3 and SDS-LDH

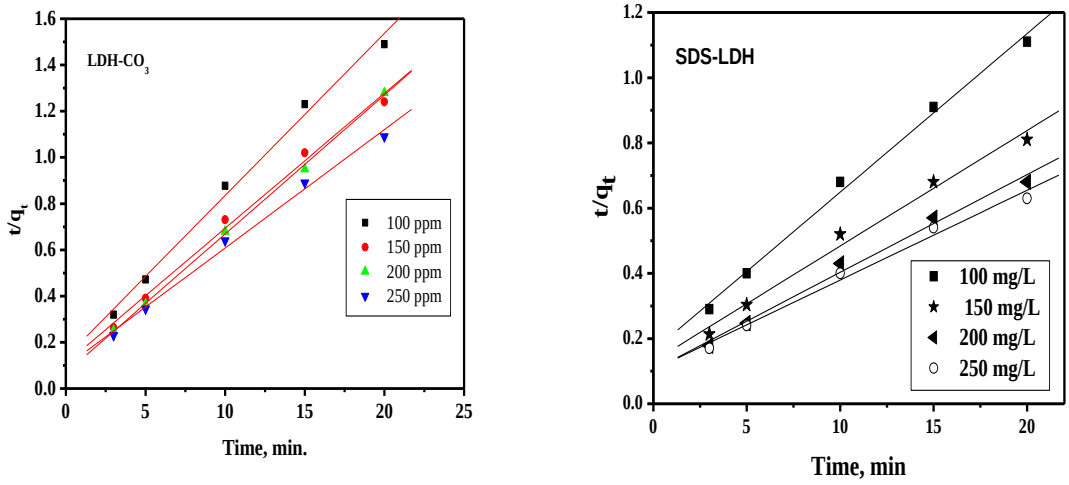

Fig. (11): Second order kinetic model for adsorption of ARS onto LDH-CO_3 and SDS-LDH

Table (1): Calculated parameters of the pseudo first-order, pseudo second-order, intra particle diffusion and Elovich kinetic models of ARS onto LDH-CO_3

Model	parameters	100, mg/L	150 mg/L	200 mg/L	250 mg/L
[LDH-CO_3]	$q_{e,\,exp.}$, (mg/g)	14.4	17.34	18.52	19.84
First-order kinetic	k_1 (min.$^{-1}$)	0.104	0.115	0.099	0.101
	$q_{e,\,calc.}$ (mg/g)	10.23	18.62	20.51	22.70
	R^2	0.980	0.947	0.974	0.960
Second-order kinetic	K_2 (min.$^{-1}$)	1.8×10^{-2}	9.42×10^{-3}	8.66×10^{-3}	6.94×10^{-3}
	$q_{e\,,calc.}$ (mg/g)	20.10	28.57	33.33	37.04
	R^2	0.994	0.980	0.990	0.986
Intra- particle diffusion	k_{id}(mg g^{-1} min$^{-0.5}$)	3.919	5.328	6.384	9.73
	C	5.975	7.857	9.571	7.019
	R^2	0.994	0.984	0.990	0.988
Elovich	a, (mg/min)	87.88	82.43	127.10	123.84
	b(g/mg^{-1})	0.524	0.391	0.415	0.383
	R^2	0.960	0.982	0.990	0.988

Table (2): Calculated parameters of the pseudo first-order, pseudo second-order, intra particle diffusion and Elovich kinetic models of ARS onto SDS-LDH

Model	parameters	100 mg/L	150 mg/L	200 mg/L	250 mg/L
[SDS-LDH]	$q_{e,\ exp.}$, (mg/g)	19.40	26.10	31.60	34.0
First-order kinetic	k1 (min.1)	0.104	0.115	0.099	0.101
	$q_{e,\ calc.}$ (mg/g)	12.59	18.62	20.42	22.70
	R^2	0.980	0.947	0.974	0.960
Second-order kinetic	K_2(min.$^{-1}$)	14.5×10^{-3}	9.64×10^{-3}	8.66×10^{-3}	6.94×10^{-3}
	$q_{e\ ,calc.}$ (mg/g)	20.57	28.25	33.33	37.04
	R^2	0.988	0.976	0.976	0.976
Intra- particle diffusion	k_{id}(mg g^{-1} min$^{-0.5}$)	3.919	5.328	6.384	7.018
	C	5.975	7.857	9.571	9.730
	R^2	0.994	0.984	0.990	0.988
Elovich	a, (mg/min)	88.15	85.97	126.97	123.84
	b(g/mg^{-1})	0.524	0.443	0.415	0.383
	R^2	0.960	0.962	0.962	0.966

The intraparticle diffusion model assumes that the adsorption process is diffusion-controlled. The intra-particles diffusion model is expressed by the following equation**:**

$$q_t = k_i t^{1/2} + C \qquad \textbf{(5)}$$

Where k_i (mg g^{-1} min$^{-0.5}$) is the intra-particle diffusion rate constant and C is the intercept which is proportional to the boundary layer thickness. The plots of q (mg /g) against $t^{0.5}$, Fig. 12 gives a linear relationships that do not pass through the origin point This indicates that the intraparticle diffusion is not the dominant mechanism in processes occurring during the sorption of Alizarine Red -S ions and the parameters are listed in Table (1, 2).

Elovich model describes the activated chemisorption. In Elovich equation

$$q_t = 1/b\ \ln(ab) + 1/b\ \ln t \qquad \textbf{(6)}$$

where a and b are constants. The constant a is considered as the initial sorption rate (mg/g min) and (b) is a constant characteristic of the process, Fig.13, the values of a and b are listed in Table (1,2). The regression coefficient (R^2) in that model is less than that of both the pseudo- first and second order models for the two investigated adsorbents which indicates that this model does not fit the data obtained.

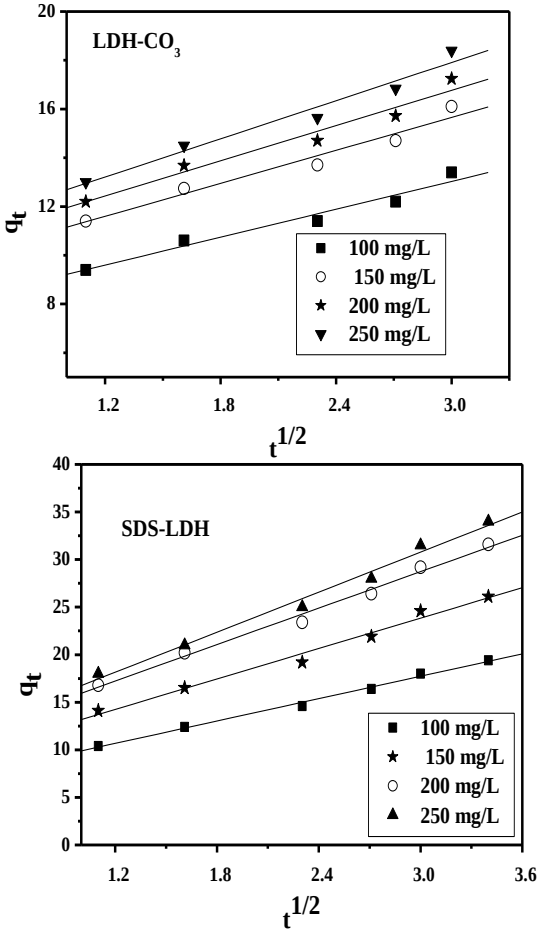

Fig. (12): The intraparticle diffusion kinetic model for the adsorption of ARS onto LDH-CO_3 and SDS-LDH

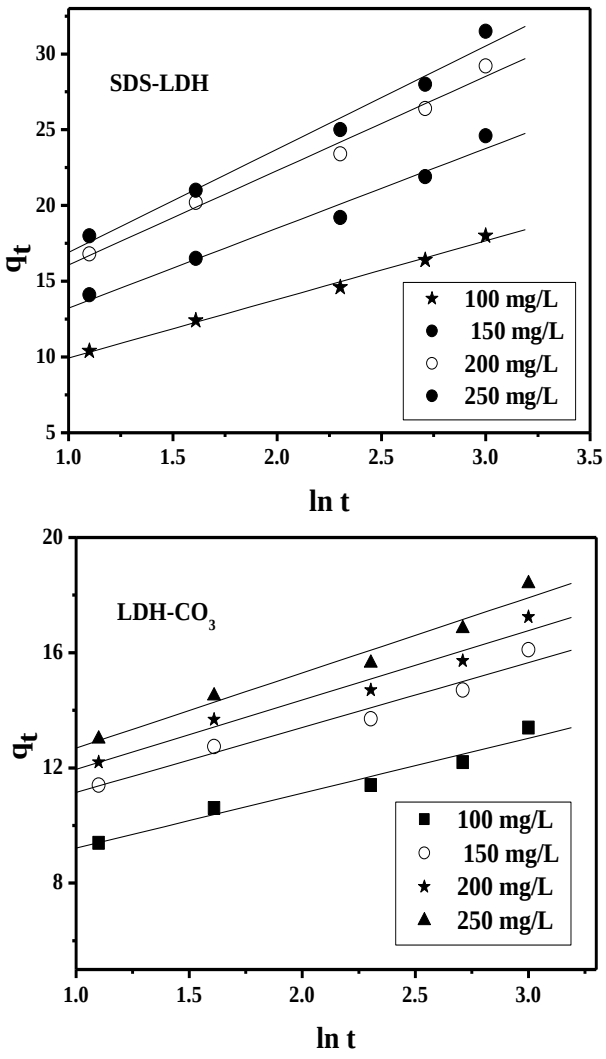

Fig. (13) Elovich kinetic model for the adsorption of ARS onto LDH-CO_3 and SDS-LDH

3.5 Effect of ARS concentration

The effect of ARS concentration on its sorption onto LDH-CO3 and SDS-LDH with a V/m ratio 200 mL/g was investigated in the range 100-250 mg/L at ambient temperature, Fig. 14. indicates that the amount of ARS sorbed onto the sorbents increased with increasing the initial dye concentration due to increasing the driving force for mass transfer with the increase in ARS concentration [54].

Langmuir and Freundlich models are commonly used to evaluate the equilibrium adsorption. In Langmuir isotherm model, the linear form is represented by the following equation:

$$\frac{C_e}{q_e} = \frac{1}{q_{max} b} + \frac{1}{q_{max}} C_e \qquad (7)$$

Where, Q_{max} is the saturated monolayer adsorption (mg/g), b is the Langmuir constant sites and is a measure of the adsorption energy mL/mg. The results are illustrated in Fig. 15 and Table (3). R_L, Langmuir isotherm is a dimensionless constant that is called equilibrium parameter and can be calculated from the following equation

$$R_L = \frac{1}{1+bC_o} \qquad (8)$$

The value of R_L was found to be $0 < R_L < 1$ that means the sorption process is favorable, Table (3).

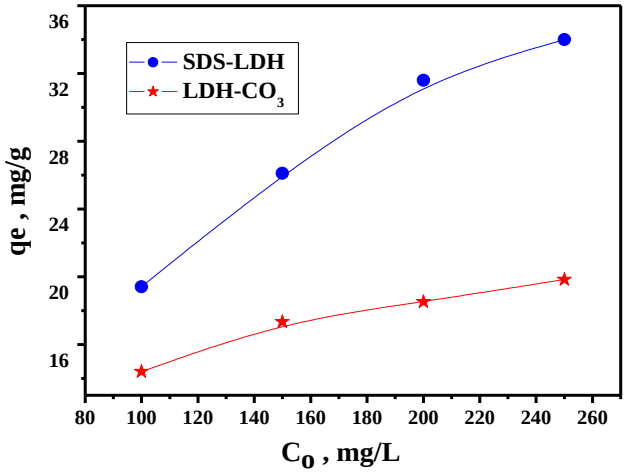

Fig. (14): Effect of initial ARS concentration on its removal onto LDH-CO_3 and SDS-LDH: V/m = 200 mL/g, pH: 6, T: 25±1°C

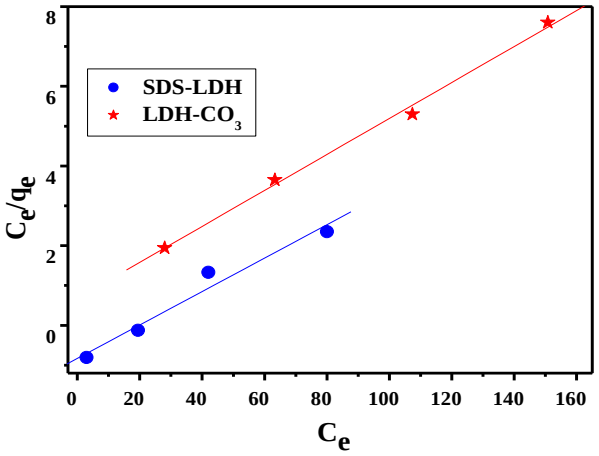

Fig. (15): Langmuir Plots for the adsorption of Alizarine Red -S onto LDH-CO_3 and SDS- LDH : V/m = 200 mL/g, pH: 6, T: 25±1°C

The Freundlich model is commonly represented as:

$$\log q_e = \log K_f + (1/n) \log Ce \qquad (9)$$

Where, K_f and n are the Freundlich constants characteristics of the system, indicating the adsorption capacity and the adsorption intensity, respectively. The plot of log q_e against log C_e is shown in Fig. 16; the value of n and K_f is tabulated in Table (3).

Table (3): Langmuir and Freundlich constants for Alizarine Red-S adsorption onto LDH-CO_3 and SDS-LDH

Model	Parameters	Value
	LDH-CO_3 adsorbent	
Langmiur	Qmax(mg/g)	22.22
	b(L/g)	0.066
	R_L	0.132
	R^2	0.996
Freundlich	1/n	0.098
	Kf (mg/g)(L/mg)$^{1/n}$	12.912
	R^2	0.996
	SDS-LSH adsorbent	
Langmiur	Qmax(mg/g)	23.87
	b(L/g)	0.05
	R_L	0.176
	R^2	0.964
Freundlich	1/n	0.173
	Kf (mg/g)(L/mg)$^{1/n}$	16.069
	R^2	0.992

In case of LDH-CO_3 system, both Langmuir and Freundlich models are applicable as the regression coefficient (R^2 around 0.996) that implies that the sorption fit the Langmuir model at low concentration and at higher concentration of the adsorbate the system obeys Freundlich model. In SDS-LDH system, Freundlich model is applicable as the regression coefficient R^2=0.992 is much higher than that obtained by Langmuir model R^2=0.964 which indicates that the dye adsorption process is affected by its own intermolecular interaction between the adsorbed dye molecules. The value of 1/n < 1 (0.17) shows favorable multilayer sorption of ARS from aqueous medium onto SDS-LDH.

A comparison of the adsorption capacity of LDH-CO_3 and SDS-LDH with other adsorbents is reported in Table 4. The results implied that LDH-CO_3 and SDS-LDH can be used efficiently for the removal of ARS from aqueous medium.

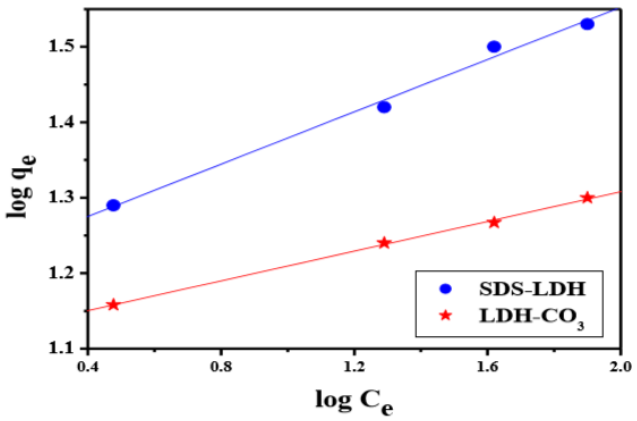

Fig. (16): Freundlich Plots for the adsorption of Alizarine Red -S onto LDH-CO_3 and SDS- LDH : V/m = 200 mL/g, pH: 6, T: 25±1°C

Table (4): Comparison of sorption capacities for Alizarine Red -S using various adsorbent materials

Sorbent	Q_{max}, mg/g	Ref.
Fe_3O_4@AMP-Tb	357.14	[52]
CS-IMBTESPEDA-SBA-15	50.25	[55]
polypyrrole-coated magnetic nanoparticles	116.30	[56]
Magnetic chitosan	40.10	[57]
Cynodondactylon	16.30	[58]
PEI@MCNTs	196.08	[59]
Activated Carbon	385.0	[60]
MCNTs	161.29	[61]
Catechol–Amine Resin-hydrocelluose composite	284.09	[62]
LDH-CO_3	22.22	This study
SDS-LDH	23.87	This study

3.6. Regeneration experiments

Desorption studies on the loaded LDH-CO_3 and SDS-LDH were carried out using 0.1M sodium hydroxide solution at 25 °C for 15 min. The desorption percentage was found to be 85 and 90% for the loaded LDH-CO_3 and SDS-LDH, respectively. In that alkaline condition, the predominant species of ARS is species 3, Fig. 6 that repel with the negative charge of the adsorbent.

4. CONCLUSION

LDH-CO_3 and intercalated SDS-LDH were investigated for the sorption of the carcinogenic, anionic dye, Alizarine Red-S to investigate the efficiency of both adsorbents for the potential removal of such dye. Intercalation with sodium dodecyl sulphate slightly improved the sorption processes. Sorption experimental data were analysed in term of kinetic models. The experimental data fitted well with the pseudo -first-order model for LDH-CO_3 and pseudo -second-order model for SDS-LDH. The adsorbents could be regenerated

through the desorption of ARS using 0.1 M NaOH solution and could be reused.

Acknowledgment

I wish to express my sincere gratitude to Prof. Dr. J. A. Daoud and Prof. Dr. H. F. Aly, Atomic Energy Authority- Egypt, for their fruitful discussions and text reviewing.

REFERENCES

[1] Calabrese, E., Kostecki, P., Dragun J. (2006) Contaminated Soils, Sediments and Water, Successes and Challenges, Vol. 10 (Springer, NY) 227-237.

[2] Rizk, S., Hamed, M. (2015) Batch sorption of iron complex dye, naphthol green B, from wastewater on charcoal, kaolinite, and tafla, Desalin Water Treat, 56, 1536–1546.

[3] Hamed M. (2014) Sorbent extraction behavior of a nonionic surfactant, Triton X-100, onto commercial charcoal from low level radioactive waste, J Radioanal. Nucl. Chem. 302, 303–313.

[4] Gharbani, P., Tabatabaii, S., Mehrizad, A. (2008) Removal of Congo Red from textile wastewater by ozonation, Int. J. Environ. Sci. Tech. 5(495), 495-500.

[5] Adyel, T., Rahman, S., Zaman, M., Hossain, M., Sayem, H., Mala, K., Abdul Gafur, Md., Islam, S. (2013) Reuse Feasibility of Electrocoagulated Metal Hydroxide Sludge of Textile Industry in the Manufacturing of Building Blocks, J.Waste. Manag. Article ID. 68698 (1) 1-9.

[6] Adyel, T., Rahman, S., Islam, S., Sayem, H., Khan, M., Zaman, M. (2012) Geo-engineering potentiality of electrocoagulated metal hydroxide sludge (EMHS) from textile industry and EMHS amended soil for using as building material, Inter J Curr Res, 4(2), 21-25.

[7] Rafaie, H., Nor, R., Azmina, M., Ramli, N., Mohamed, R. (2017) Decoration of ZnO microstructures with Ag nanoparticles enhanced the catalytic photodegradation of methylene blue dye, J Environ Chem Eng. 5 (4), 3963- 3972.

[8] Sheng, S., Liu, B., Hou, X., Wu, B., Yao, F., Ding, X., Huang, L. (2018) Aerobic Biodegradation Characteristic of Different Water-Soluble Azo Dyes, Int. J. Environ. Res. Public Health. 15(1) (2018) 35-40

[9] A. Konsowa, H. Abd El-Rahman, F. (2011) Removal of azo dye acid orange using aerobic membrane bioreactor. Alex. Eng. J. 50(1), 117-125.

[10] Waleed, M., Alabdraba, M., Aldoury, M. Bayati, M. (2014) Performance of Sequential Anaerobic/Aerobic Biological Treatment of Synthetic Wastewater Containing Two Types of Azo Dye. Conference: ICOEST'2, Turkey.

[11] Singh, S., Sidhu, G., Singh, H. (2017) Removal of methylene blue dye using activated carbon prepared from biowaste precursor, Indian Chem. Eng. 61(1), 28-39.

[12] Greluk, M., Hubicki, Z. (2011) Efficient removal of acid orange 7 dye from water using the strongly basic anion exchange resin Amberlite IRA-958, Desalination. 278 (1-3), 219-226

[13] Shao, J., Cheng, Y., Yang, C., Zeng, G., Liu, W., Jiao, P., He, H. (2016) Efficient removal of naphthalene-2-ol from wastewater by solvent extraction, J. Environ. Sci. 47(9),120-129

[14] Chen, G., Lei, L.,Yue, P. (1999) Wet oxidation of high-concentration reactive dyes, Ind. Eng. Chem. Res. 38, 1837-1843.

[15] Tan, B., Teng, T., Omar, A. (2000) Removal of dyes and industrial dye wastes by magnesium chloride, Water Res. 34(2) 597-600.

[16] Park, Y., Ayoko, G., Frost, R. (2011) Application of organoclays for the adsorption of recalcitrant organic molecules from aqueous media, J. Colloid Interface Sci. 354, 292-305J.

[17] Baptisttella, A., Araújo, A., Barreto, M., Motta, M. (2018)The use of metal hydroxide sludge (in natura and calcined) for the adsorption of brilliant blue dye in aqueous solution. Environ Technol 40(2),1-35.

[18] Attallah, M., Ahmed, I.M., Hamed, M. (2013) Treatment of industrial wastewater containing Congo Red and Naphthol Green B using low-cost adsorbent, ESPR. 20, 1106-1116.

[19] Xue, S., Zhu, F., Kong, X., Wu, C., Huang, L., Huang, N., Hartley, W. (2016) A review of the characterization and revegetation of bauxite residues (Red mud), Environ. Sci. Pollut. R. 23, 1120-1132.

[20] Yalçın, N., Sevinç, V. (2000) Utilization of bauxite waste in ceramic glazes, Ceramics Inter. 26 (5), 485-493

[21] Tor, A., Cengeloglu, Y. (2006) Removal of congo red from aqueous solution by adsorption onto acid activated red mud, J. Hazard. Mater. B.138, 409-415.

[22] Fu, F., Dionysioub, D., Liu, H. (2014) The use of zero-valent iron for groundwater remediation and wastewater treatment: A review, J. Hazard. Mater. 267, 194-205.

[23] Narbaitz, R., Karimi-Jashni, A. (2009) Electrochemical regeneration of granular activated carbons loaded with phenol and natural organic matter. Environ. Technol., 30, 27-36.

[24] Adeyemo, A., Adeoye, I., Bello, O. (2017) Adsorption of dyes using different types of clay: a review. Appl. Water Sci.7, 543-568.

[25] Argun, Y., Tunç, A., Çalışır, U., Irak, H. (2017) Bisorption method and biosorptions for dye removal from industrial wastewater: A Review, Inter. J. Adv. Res.5(8),707-714.

[26] Pushpa, T., Jegan, J., Saravanan, P., Ravindiran, G. (2019) Biodecolorization of Basic Blue 41 using EM based Composts: Isotherm and Kinetics. Chem. Select 4(34), 10006 -10012.

[27] Karim, Md., Dhar, K., Hossain, Md. (2016) Co-metabolic decolorization of a textile reactive dye by Aspergillus fumigatus. Inter. J. Environ. Sci. Technol. 14,177-186.

[28] Trifiro, F., Vaccari, A. (1996) Oxford, UK: Pergamon Press Hydrotalcite-like anionic clays (Layered double hydroxides). In: Davies, J. E. D., Atwood, J. L., MacNicol, D. Vogtle, F. (Eds), Comprehensive Supramolecular Chemistry, Oxford, UK: Pergamon Press, p.251-291.

[29] Ahmed, I.M., Gasser, M. (2012) Adsorption Study of Anionic Reactive Dye from Aqueous Solution to Mg-Fe-CO_3 Layered Double Hydroxide (LDH). Appl. Surf. Chem. 259, 650-656.

[30] Kameda, T., Takeuchi, H., Yoshioka, T. (2008) Uptake of heavy Alizarine Red-S from aqueous solution using Mg-Al layered double hydroxides intercalated with citrate, malate, and tartrate, Separ. Purif. Technol. 62(2), 330-336.

[31] Kameda, T., Takeuchi, H.,Yoshioka, T. (2015) Uptake of $Nd^{3+}$and Sr^{2+} by Li-Al layered double hydroxide intercalated with triethylenetetramine-hexaacetic acid: kinetic and equilibrium studies, RSC Adv. 5, 79447-79455.

[32] Kameda, T., Takeuchi, H., Yoshioka, T. (2016) Uptake of Nd^{3+} and Sr^{2+} by LiAl layered double hydroxides intercalated with ethylenediaminetetraacetate, Mater. Chem. Phys. 177, 8-11.

[33] Koilraj, P., Kamura, Y., Sasaki, K. (2017) Carbon-dot-decorated layered double hydroxide nanocomposites as a multifunctional environmental material for Coimmobilization of SeO_4^{2-} and Sr^{2+} from aqueous solutions, ACS Sustain. Chem. Eng. 5(10), 9053-9064.

[34] Yao, W., Yu, S., Wang, J., Zou, Y., Lu, S., Ai, Y., Alharbi, N., Alsaedi, A., Hayat, T.,Wang, X. (2017) Enhanced removal of methyl orange on calcined glycerol-modified nanocrystallined Mg/Al layered double hydroxides, Chem. Eng. J., 307, 476-486.

[35] Aguiar, J., Bezerra, B., Braga, B., Lima, P., Nogueira, R., Lucena, S., Da Silva, I. (2013)Adsorption of Anionic and Cationic Dyes from Aqueous Solution on Non-Calcined Mg-Al Layered Double Hydroxide: Experimental and Theoretical Study, Sep. Sci. Technol. 248, 2307-2316.

[36] Pahalagedara, M., Samaraweera, M., Dharmarathna, S., Kuo, C., Pahalagedara, L., Gascón, J Suib, S. (2014) Removal of Azo Dyes: Intercalation into Sonochemically Synthesized NiAl Layered Double Hydroxide, J. Phys. Chem. *C* 118(31), 17801-17809.

[37] Blaisi, N., Zubair, M., Ihsanullah, M., Ali, S., Kazeem, T., Manzar, M., Al-Kutti, W., Al Harthi, M. (2018) Date palm ash-MgAl-layered double hydroxide composite: sustainable adsorbent for effective removal of methyl orange and eriochrome black-T from aqueous phase, Environ Sci Pollut Res Int. Environ. Sci. Pollut. Res. Int., 25(34), 34319-34331.

[38] Tan, X., Liu, Y., Gu, Y., Liu, S., Zeng, G., Cai, X., Hu, X., Wang, H., Liu, S., Jiang, L. (2016) Biochar pyrolyzed from MgAl-layered double hydroxides pre-coated ramie biomass (Boehmeria nivea (L .) Gaud .): Characterization and application for crystal violet removal, J. Environ. Manage. 15(184), 1-9.

[39] Zhu, L. Chen, T. Yan, J. Xu, Y. Wang, M. Chen, H. Jiang, F. (2018) Fabrication of Fe_3O_4/MgAl-layered double hydroxide magnetic composites for the effective removal of Orange II from wastewater, Water Sci Technol. 78(5-6),1179 -1188.

[40] Dizge, N., Aydiner, C., Demirbas, E., Kobya, M., Kara,S. (2005)Adsorption of reactive dyes from aqueous solutions by fly ash: kinetic and equilibrium studies, J Hazard. Mater.150(3), 737-46

[41] Safavi, A., Bagheri, M. (2005) A novel optical sensor for uranium determination, Analytica Chimica Acta. 530(1), 155-160 .

[42] Hernández, J., Méndez, B., Cordero, M., Gutierrez, L., Dávila, L. (1985) Spectrophotometric determination of zirconium with alizarin red S in the presence of polyvinylpyrrolidone. Analytica Chimica Acta. 175, 345-348.

[43] Leng, S.F., Jing , Y., Wei , Q., Wang, Y., Lv, Y., Wang, X., Zhu, X. (2016) Spectrophotometric method for determination of trace aluminum with application of Alizarin Red. Bulgarian Chemical Communications, 48(1),159-164.

[44] Mahmoud, M., Someda, H. (2012) Mg-Al layered double hydroxide intercalated with sodium lauryl sulfate as a sorbent for $^{152+154}$Eu from aqueous solutions. J. Radioanal. Nucl. Chem . 292,1391-1400.

[45] Moriguchi, T.,Yano, K., Nakagawa, S., Kaji, F. (2003) Elucidation of adsorption mechanism of bone-staining agent alizarin red Son hydroxyapatite by FT-IR microspectroscopy J. Colloid Interface Sci. 260,19-25.

[46] Millange, F., Walton, R.I., D. O'Hare, D. (2000) Time-resolved in situ X-ray diffraction study of the liquid-phase reconstruction of Mg^{2+}-Al^{3+}- carbonate hydrotalcite-like compounds. J. Mater. Chem. 10, 1713-1720.

[47] Ahmed, I. M. and Gasser, M.S. (2012) Adsorption Study of Anionic Reactive Dye from Aqueous Solution toMg-Fe-CO_3 Layered Double Hydroxide (LDH), Appl. Surf. Chem., 259, 650-656.

[48] Mandal, S., Tripathy, S., Padhi, T., Sahu, M., Patel, R. (2013) Removal efficiency of fluoride by novel Mg-Cr-Cl layered double hydroxide by batch process from water, J. Environ. Sci. 25(5), 993-1000.

[49] Hamed, M., Ahmed, I.M., Metwally, S. (2014) Adsorptive removal of methylene blue as organic pollutant by marble dust as eco-friendly sorbent, J Ind Eng Chem 20(4), 2370-2377.

[50] Ahmed, I.M., Aglan, R., Hamed., M. (2017) Removal of Arsenazo-III and Thorin from radioactive waste solutions by adsorption onto low-cost adsorbent, J. Radioanal. Nucl. Chem. 314, 2253-2262.

[51] Turcanu, A., Bechtold,T. (2011) pH Dependent redox behaviour of Alizarin Red S (1,2-dihydroxy-9,10-anthraquinone-3-sulfonate) – Cyclic voltammetry in presence of dispersed vat dye, Dyes and Pigments. 91(3), 324-331.

[52] Huanga, W., Deng, J., Zhou, T., Lu, D., Shi, G., Xu, J. (2018) Rational design of magnetic infinite coordination polymer core-shell nanoparticles as recyclable adsorbents for selective removal of anionic dyes from colored wastewater, Appl. Surf. Sci. 462, 453-465.

[53] Ahmed, I.M., Attia, L., Attallah. M. (2020) Modification of perlite to prepare low cost zeolite as adsorbent material for removal of ^{144}Ce and$^{152+154}$Eu from aqueous solution, Radiochim. Acta. https://doi.org/10.1515/ract-2019-3221.

[54] Metwally, S., Ayoub, R., Aly, H.F. (2014) Utilization of low-cost sorbent for removal and separation of ^{137}Cs, ^{60}Co and $^{152+154}$Eu radionuclides from aqueous solution, J. Radioanal. Nucl. Chem. 302, 441-449.

[55] Pourebrahim, F., Ghaedi, M., Dashtian, K., Heidari, F., Kheirandish, S. (2017) Simultaneous removing of Pb^{2+} ions and alizarin red S dye after their complexation by ultrasonic waves coupled adsorption process: Spectrophotometry detection and optimization study, Ultrason. Sonochem. 35, 51-60.

[56] Gholivand, M., Yamini, Y., Dayeni, M., Seidi, S., Tahmasebi, E. (2015) Adsorptive removal of alizarin red-S and alizarin yellow GG from aqueous solutions using polypyrrole-coated magnetic nanoparticles. J. Environ. Chem. Eng. 3(1), 529-540.

[57] Fan, L., Zhang, Y., Li, X., Luo, C., Lu, F., Qiu, H. (2012) Removal of alizarin red from water environment using magnetic chitosan with alizarin red as imprinted molecules. Colloids Surf B: Biointerfaces.91, 250-257.

[58] Samusolomon, J., Devaprasath, P.M. (2011) Removal of Alizarin Red S (Dye) from Aqueous Media by using Cynodon dactylon as an Adsorbent, J. Chem. Pharm, Res, 3, 478-490.

[59] Zhang, Z., Chen, H., Wu, W., Pang, W., Yan, G. (2019) efficient removal of Alizarin Red S from aqueous solution by polyethyleneimine functionalized magnetic carbon nanotubes. Biores. Technol. 293, 122100.

[60] Benhmidene, A., Hidouri, K., Amor, H., Chaouachi, B. (2017) Kinetic Models of Adsoption on Active Carbon, DSAC36-24 Global J. Res Eng.: C Chem. Eng. 17(3), 1-10.

[61] Ghaedi, M., Hassanzadeh, A., Kokhdan, S. (2011) Multiwalled Carbon Nanotubes as Adsorbents for the Kinetic and Equilibrium Study of the Removal of Alizarin Red S and Morin, J. Chem. Eng. Data. 56(5), 2511-2520.

[62] Liu, Q., Wu, Z., Wu, Y., Gao, T., Yao, J. (2107) Efficient Removal of Methyl Orange and Alizarin Red S from pH-Unregulated Aqueous Solution by the Catechol–Amine Resin Composite Using Hydrocellulose as Precursor, CS Sustainable Chem. Eng. 5(2), 1871-1880.